British Journal of Pharmacology

DOI:10.1111/bph.13314
www.brjpharmacol.org

RESEARCH PAPER

Putative binding sites for arachidonic acid on the human cardiac $K_v1.5$ channel

Jia-Yu Bai[1]*, Wei-Guang Ding[1]*, Akiko Kojima[2], Tomoyoshi Seto[2] and Hiroshi Matsuura[1]

[1]*Department of Physiology, Shiga University of Medical Science, Otsu, Japan, and* [2]*Department of Anesthesiology, Shiga University of Medical Science, Otsu, Japan*

Correspondence
Hiroshi Matsuura, Department of Physiology, Shiga University of Medical Science, Otsu, Shiga 520-2192, Japan.
E-mail: matuurah@belle.shiga-med.ac.jp
*These authors made equal contribution to this study.

Received
30 April 2015
Revised
1 August 2015
Accepted
18 August 2015

BACKGROUND AND PURPOSE

In human heart, the $K_v1.5$ channel contributes to repolarization of atrial action potentials. This study examined the electrophysiological and molecular mechanisms underlying arachidonic acid (AA)-induced inhibition of the human $K_v1.5$ ($hK_v1.5$) channel.

EXPERIMENTAL APPROACH

Site-directed mutagenesis was conducted to mutate amino acids that reside within the pore domain of the $hK_v1.5$ channel. Whole-cell patch-clamp method was used to record membrane currents through wild type and mutant $hK_v1.5$ channels heterologously expressed in CHO cells. Computer docking simulation was conducted to predict the putative binding site(s) of AA in an open-state model of the $K_v1.5$ channel.

KEY RESULTS

The $hK_v1.5$ current was minimally affected at the onset of depolarization but was progressively reduced during depolarization by the presence of AA, suggesting that AA acts as an open-channel blocker. AA itself affected the channel at extracellular sites independently of its metabolites and signalling pathways. The blocking effect of AA was attenuated at pH 8.0 but not at pH 6.4. The blocking action of AA developed rather rapidly by co-expression of $K_v\beta1.3$. The AA-induced block was significantly attenuated in H463C, T480A, R487V, I502A, I508A, V512A and V516A, but not in T462C, A501V and L510A mutants of the $hK_v1.5$ channel. Docking simulation predicted that H463, T480, R487, I508, V512 and V516 are potentially accessible for interaction with AA.

CONCLUSIONS AND IMPLICATIONS

AA itself interacts with multiple amino acids located in the pore domain of the $hK_v1.5$ channel. These findings may provide useful information for future development of selective blockers of $hK_v1.5$ channels.

Abbreviations

AA, arachidonic acid; AF, atrial fibrillation; APD, action potential duration; BIS-I, bisindolylmaleimide I; COX, cyclooxygenase; ERP, effective refractory period; ETYA, 5,8,11,14-eicosatetraynoic acid; HERG, human *ether-a-go-go*-related gene; IDM, indomethacin; I_{Kur}, ultra-rapid delayed rectifier potassium current; LOX, lipoxygenase; NDGA, nordihydroguaiaretic; PKC, protein kinase C; SOD, superoxide dismutase; WT, wild type

Tables of Links

TARGETS	
Ion channels[a]	**Enzymes**[b]
Kv1.2	COX
Kv1.5	Cytochrome P450
	LOX
	PKC
	PLA2

LIGANDS
Arachidonic acid (AA)
Bisindolylmaleimide 1 (BIS-1)
ETYA
Indomethacin
NDGA

These Tables list key protein targets and ligands in this article which are hyperlinked to corresponding entries in http://www.guidetopharmacology.org, the common portal for data from the IUPHAR/BPS Guide to PHARMACOLOGY (Pawson *et al.*, 2014) and are permanently archived in the Concise Guide to PHARMACOLOGY 2013/14 ([a,b]Alexander et al., 2013a,b).

Introduction

Arachidonic acid (AA; 20:4, n-6) is a *cis*-polyunsaturated fatty acid that is ubiquitously present in the plasma membrane. AA is liberated through the activation of PLA_2. AA exerts its various biological actions on ion channels through different mechanisms: either the AA molecule itself or through AA metabolites that are produced by the cyclooxgenase (COX), lipoxygenase (LOX) and cytochrome P450 pathways (Brash, 2001; Meves, 2008). In addition, some of the effects of AA on ion channels are mediated through protein kinase C (PKC) and oxygen radicals (Linden and Routtenberg, 1989; Keyser and Alger, 1990). The intracellular and extracellular levels of AA have been reported to increase in several patho-physiological conditions, such as myocardial ischaemia (Chien *et al.*, 1984), hypoxia (McHowat *et al.*, 1998) and inflammation (Yedgar *et al.*, 2006). It is noteworthy that AA can also be quickly produced in response to cytokines such as IL-1β and TNF-α from rat ventricular cells (Liu and McHowat, 1998).

A number of studies have investigated the effects of AA on cardiac ion channels; these were either native ion channels in cardiac myocytes of experimental animals or human ion channels heterologously expressed in cultured cell lines. For example, AA inhibits the L-type Ca^{2+} channel in ventricular myocytes of frogs and rats (Petit-Jacques and Hartzell, 1996; Liu, 2007) and the G protein-gated K^+ channel (Kim and Pleumsamran, 2000) in rat cultured atrial myocytes. AA also suppresses human T-type Ca^{2+} channel ($Ca_V3.1$, α_{1G}) and human *ether-a-go-go*-related gene (HERG) K^+ channel, heterologously expressed in cultured cell lines (Talavera *et al.*, 2004; Guizy *et al.*, 2005). In contrast, AA activates the ATP-sensitive K^+ channel in rat ventricular myocytes (Lu *et al.*, 2006) and human inwardly rectifying K^+ channel $K_{ir}2.3$ heterologously expressed in CHO cells (Liu *et al.*, 2001). However, AA has no effect on human $K_{ir}2.1$, $K_{ir}2.2$ or $K_{ir}2.4$ channels (Liu *et al.*, 2001). Thus, AA produces different effects on cardiac ion channels, depending on the types of ion channels.

The human $K_V1.5$ (hKv1.5) channel is encoded by the *KCNA5* gene and underlies the ultra-rapid delayed rectifier K^+ current (I_{Kur}) in the heart (Fedida *et al.*, 1993; Wang *et al.*, 1993; Mays *et al.*, 1995). I_{Kur} is rapidly activated following the upstroke of action potentials and provides outward currents to repolarize the cell membrane (Ravens and Cerbai, 2008). In the human heart, the $hK_V1.5$ channel is predominantly expressed in atrium but sparsely in ventricle (Feng *et al.*, 1997). I_{Kur} has received much attention as a potentially promising molecular target for the prevention and treatment of re-entry-based atrial fibrillation (AF), as the blockade of I_{Kur} is expected to selectively prolong the action potential duration (APD) and effective refractory period (ERP) in the atrium without the risk of excessive prolongation of ventricular repolarization in humans (Ravens and Wettwer, 2011). In fact, a previous report showed that the pharmacological blockade of $hK_V1.5$ prolongs APD in atrial trabeculae isolated from patients with AF (Wettwer *et al.*, 2004).

In an early study it was clearly shown that relatively high concentrations of AA (IC_{50} of 21 μM) inhibit the mouse $K_V1.5$ ($mK_V1.5$) channel and that AA metabolites are not involved in this effect (Honoré *et al.*, 1994). However, the molecular mechanism underlying this channel inhibition has not been fully elucidated. Previous site-directed mutagenesis studies of the $hK_V1.5$ channel have indicated that several of the amino acids that reside within the pore region act as putative binding sites for various pharmacological inhibitors (Yeola *et al.*, 1996; Decher *et al.*, 2004; Decher *et al.*, 2006; Eldstrom et al., 2007; Wu *et al.*, 2009; Ravens and Wettwer, 2011). The present study was designed to investigate the molecular determinants that underlie the AA-induced inhibition of $hK_V1.5$ using site-directed mutagenesis combined with patch-clamp experiments, in addition to computer docking simulations with an open-state model of the $K_V1.5$ channel. We found that several amino acids in the pore domain (H463, T480, R487, I502, I508, V512 and V516) are involved in mediating the blocking action of AA on $hK_V1.5$ channels.

Methods

Cell culture and site-directed mutagenesis

CHO cells were maintained in DMEM/Ham's F-12 supplemented with 10% FBS and antibiotics (100 $IU \cdot mL^{-1}$ penicillin and 100 $\mu g \cdot mL^{-1}$ streptomycin) in an incubator gassed with 5% CO_2 and 95% air at 37°C. The full-length complementary

DNA (cDNA) of the hK$_v$1.5 channel was subcloned into the mammalian expression vector pcDNA3 (kindly provided by Dr D. Fedida; University of British Columbia, Canada).

PCR-based site-directed mutagenesis was applied to introduce 11 single point mutations (T462C, H463C, T479A, T480A, R487V, A501V, I502A, I508A, L510A, V512A and V516A) into hK$_v$1.5 cDNA by using a Quikchange-II-XL Kit (Agilent Technologies, Santa Clara, CA, USA). All products were fully sequenced using an ABI PRISM-3130 sequencer (ABI3100x/, Applied Biosystems, Foster City, CA, USA) to ensure the fidelity of the PCR reactions. Wild type (WT) and mutant cDNA were transiently transfected into CHO cells together with GFP cDNA using Lipofectamine (Invitrogen Life Technologies, Carlsbad, CA, USA). After transfection for 48 h, the GFP-positive cells were used for the patch-clamp experiments.

Solutions and chemicals

The bath solution for whole-cell recording contained (in mM): 140 NaCl, 5.4 KCl, 1.8 $CaCl_2$, 0.5 $MgCl_2$, 0.33 NaH_2PO_4, 5.5 glucose and 5.0 HEPES, and pH was adjusted to 7.4 with NaOH. For experiments in acidic (pH 6.4) or alkaline conditions (pH 7.7 and 8.0), pH of bath solution was adjusted with HCl or NaOH respectively. AA (Sigma Chemical Co., St Louis, MO, USA) was dissolved in DMSO to make a stock solution of 20–50 mM. Indomethacin (IDM, Sigma), nordihydroguaiaretic acid (NDGA, Sigma), 5,8,11,14-eicosatetraynoic acid (ETYA, Sigma) and bisindolylmaleimide I (BIS-I, Sigma) were dissolved in DMSO to make the stock solution. The final concentration of DMSO used in the present experiments was less than 0.1%, which had no effect on hK$_v$1.5 currents. Superoxide dismutase (SOD, Sigma) was dissolved in deionized water (stock solution, 30 000 U·mL^{-1}). Fatty acid-free BSA (Sigma) was directly dissolved in the bath solution. The pipette solution contained (in mM): 70 potassium aspartate, 40 KCl, 10 KH_2PO_4, 1 $MgSO_4$, 3 Na_2-ATP (Sigma), 0.1 Li_2-GTP (Roche Diagnostics GmbH, Mannheim, Germany), 5 EGTA and 5 HEPES, and pH was adjusted to 7.2 with KOH.

Whole-cell patch-clamp recordings and data analysis

Whole-cell membrane currents were recorded with an EPC-8 patch-clamp amplifier (HEKA, Lambrecht, Germany). Data were low-pass filtered at 1 kHz and acquired at 5 kHz through an LIH-1600 AD/DA interface (HEKA) using PULSE/PULSEFIT software (HEKA). Patch electrodes were fabricated from glass capillaries (Narishige Scientific Instrument Lab, Tokyo, Japan) using a P-97 horizontal puller (Sutter Instrument, Novato, CA, USA) and had a resistance of 2.0–3.0 MΩ when filled with the pipette solution. A coverslip with adherent CHO cells was placed on the glass bottom of a recording chamber (0.5 mL in volume) and continuously perfused at a rate of 2 mL·min^{-1} with bath solution at 25°C. The hK$_v$1.5 currents were activated by applying 300 ms depolarizing voltage-clamp steps from a holding potential of −80 mV to various test potentials of −50 to +50 mV in 10 mV steps with a return potential of −40 mV. The zero current level is indicated by the horizontal bar to the left of current traces. The concentration–response relationship for the inhibitory action of AA on hK$_v$1.5 was drawn according to the least-squares fit of Hill equation: % of control = $100/(1+([\text{drug}]/IC_{50})^{nH})$ where IC_{50} is the concentration of AA causing a half-maximal inhibition and n_H is Hill coefficient. Data for the voltage-dependence of hK$_v$1.5 activation was fitted with a Boltzmann equation: $I_{tail} = 1/(1+\exp((V_{1/2}-V_m)/k))$ where I_{tail} is the tail current amplitude normalized with reference to the maximum value measured at +50 mV, $V_{1/2}$ is the half-maximal voltage, V_m is the test potential and k is the slope factor. In addition, the channel deactivation kinetics was determined by fitting a single exponential function to the tail current trace.

Docking simulation study for AA binding to the K$_v$1.5 channel model

The hK$_v$1.5 modelling, AA docking and three-dimensional representation were performed using the Molecular Operating Environment (MOE) 2014.0901 (Chemical Computing Group, Inc., Quebec, Canada). An open-state homology model of the K$_v$1.5 channel was obtained from the modelling software MOE-Homology Model using the 2.9 Å crystal structure of the Kv1.2 channel (Protein Data Bank: 2A79) (Long *et al.*, 2005) as a template, which is approximately 90% homologous in the pore domain with hK$_v$1.5. AA was docked to the K$_v$1.5 model using the ASEDock2013.11.14 program (Ryoka Systems Inc., Tokyo, Japan) (Goto *et al.*, 2008). Briefly, ASEDock is a docking programme that uses shape similarity assessments between the concave portion (i.e. concavity) of a protein and its ligand, to search for the structures of ligand–receptor complexes. All of the receptor atoms were fixed for docking. The ASEDock programme treats the ligands as flexible molecules. The programme allows the rotatable bonds of the ligands to produce conformers (1000 conformers were generated for AA) that fit to the binding region of the receptor, while it conserves the configuration of the chiral centres. We adopted the MMFF94s force field (Halgren, 1996; Halgren, 1999) to set partial charge and force-field parameters and then calculated the AA binding energy to the fixed K$_v$1.5 model. The total binding energy and its components, namely, electrostatic, van der Waals and ligand energy, were calculated by molecular mechanics using the MOE. The minimum binding energy was used to identify the AA docking to the channel.

Statistical analysis

All data were expressed as mean ± SEM. Statistical comparisons between two groups were analysed using Student's *t*-test. Comparisons among multiple groups were analysed using one-way ANOVA, followed by Dunnett's *post hoc* test, and a P value < 0.05 was considered significant.

Results

Concentration-dependent inhibition of hK$_v$1.5 current by AA

The hK$_v$1.5 current was elicited every 10 s by applying 300 ms depolarizing voltage-clamp steps to +30 mV, before (control) and during exposure to increasing concentrations (between 0.2 to 20 μM) of AA in a cumulative manner (Figure 1A). AA at concentrations of ≥1 μM appreciably inhibited the hK$_v$1.5 current,

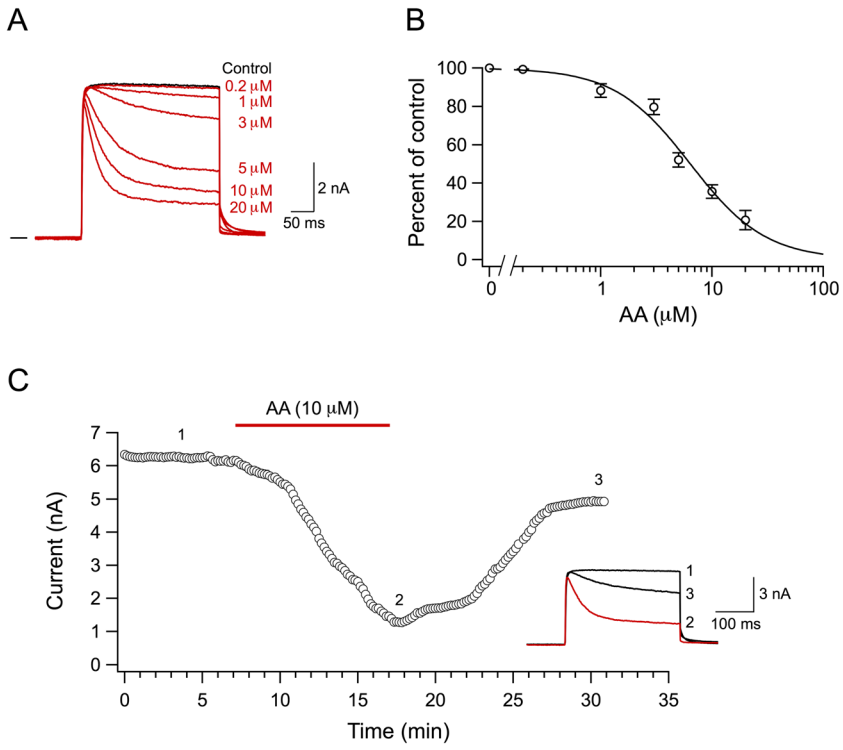

Figure 1

Concentration-dependent inhibitory effect of AA on $hK_v1.5$ current. (A) Superimposed $hK_v1.5$ current traces during 300 ms depolarizing voltage-clamp steps applied from a holding potential of −80 mV to a test potential of +30 mV, before (control) and during exposure to increasing concentrations (0.2, 1, 3, 5, 10 and 20 μM) of AA. AA was added in a cumulative manner after inhibition by the previous concentration reached a steady state. (B) Concentration–response relationship for the inhibitory action of AA on the $hK_v1.5$ current. The % of control represents the fraction of the current in the presence of each concentration of AA with reference to the control amplitude, measured at the end of a depolarizing step to +30 mV. The smooth curve through the data points (mean ± SEM, $n = 10$) represents a least-squares fit of a Hill equation, yielding an IC_{50} of 6.1 ± 0.6 μM and n_H of 1.3 ± 0.2. (C) Changes in the amplitude of $hK_v1.5$ current, activated by 300 ms depolarizing step to +30 mV from a holding potential of −80 mV, before, during the application of AA (10 μM) and after its washout. The period of AA application is indicated by the horizontal bar.

which was characterized by a more potent reduction of late current levels in comparison with initial current levels during depolarizing voltage-clamp steps. This observation suggests that AA preferentially affects the open state of the channels (acts as an open-channel blocker). Figure 1B illustrates the mean concentration–response relationship for the reduction in the $hK_v1.5$ current induced by AA, measured at the end of the depolarizing steps to +30 mV. The data were reasonably well fitted with a Hill equation with an IC_{50} of 6.1 ± 0.6 μM and n_H of 1.3 ± 0.2 ($n = 10$). Figure 1C illustrates the time course of changes in the amplitude of the $hK_v1.5$ current during the application of the submaximally effective concentration (10 μM) of AA. The inhibitory effect of AA reached a maximum at about 10 min after the application of AA, which was largely reversed after the washout of AA (restored to 82.6 ± 4.1% of its initial control value).

Blocking properties of AA on the $hK_v1.5$ current

Figure 2A demonstrates superimposed current traces of the $hK_v1.5$ current during depolarizing voltage-clamp steps applied from a holding potential of −80 mV to test potentials of −50 to +50 mV before (control) and approximately 10 min after exposure to 10 μM AA. Under control conditions, the $hK_v1.5$ current was appreciably activated at test potentials of greater than or equal to −20 mV. The bath application of AA induced a time-dependent decline in the outward currents during the depolarizing steps, which appeared to be more pronounced at stronger depolarizations. Figure 2B illustrates *I–V* relationships for late current levels (measured at the end of depolarizing steps) before and during the application of AA. We also analysed the voltage-dependent activation of $hK_v1.5$ channels in the absence and presence of AA by fitting a Boltzmann equation to the amplitudes of tail currents elicited at −40 mV after depolarizing voltage steps to various levels (Figure 2C). In a total of 17 cells, $V_{1/2}$ averaged −7.0 ± 1.4 mV in control and −28.9 ± 1.9 mV ($P < 0.01$) in the presence of AA, while k was 11.6 ± 1.0 mV in control and 5.1 ± 1.1 mV ($P < 0.01$) in the presence of AA. This hyperpolarizing shift of $V_{1/2}$ combined with steeper slope (as represented by smaller k) by AA can be explained as follows: because the degree of $hK_v1.5$ inhibition by AA was small at weak depolarizations and became large with strong depolarizations (see also Figure 2D), tail current amplitude measured at weak depolarizations relative to that at +50 mV became larger in

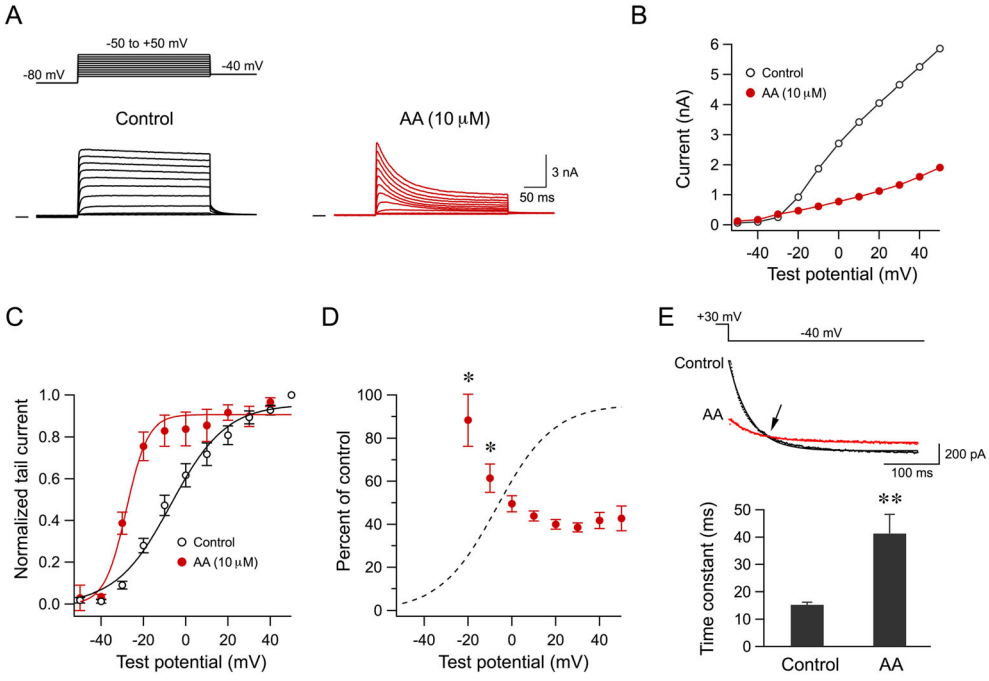

Figure 2

Blocking properties of AA on hK$_v$1.5 channel. (A) Superimposed hK$_v$1.5 currents elicited during 300 ms depolarizing steps given from a holding potential of −80 mV to test potentials of −50 and +50 mV in 10 mV steps, before (left panel) and 10 min after exposure to 10 μM AA (right panel). (B) *I–V* relationships of the late currents measured at the end of depolarizing steps in control and during exposure to AA, obtained from the data shown in panel A. (C) *I–V* relationships for the peak amplitudes of tail currents elicited at −40 mV following depolarizing steps to −50 through +50 mV in control and during exposure to 10 μM AA. The amplitudes of peak tail currents at test potentials were normalized with reference to the amplitude at +50 mV in each condition. The smooth curves through the data points represent a least-squares fit of a Boltzmann equation. (D) The amplitude of the late current during depolarizing step in the presence of AA is plotted as % of control amplitude measured in the absence of AA (mean ± SEM, $n = 10$). The dashed curve represents the activation curve obtained in control conditions (C). *$P < 0.05$ compared with the value at +50 mV. (E) The crossover of tail current traces recorded in the absence and presence of AA. Upper panel: tail currents (dotted points) recorded at −40 mV after depolarizing step to +30 mV in control and during exposure to 10 μM AA, fitted with a single exponential function (continuous curve). The arrow denotes a crossover of tail currents. Lower panel: time constants for deactivation of hK$_v$1.5 current measured at −40 mV after depolarization to +40 mV before (control) and during exposure to AA. **$P < 0.01$ compared with control.

the presence of AA compared with control conditions. Similar changes in $V_{1/2}$ and k have been noted in other open-channel blockers of hK$_v$1.5, such as mibefradil (Perchenet and Clément-Chomienne, 2000) and LY294002 (Wu *et al.*, 2009).

To examine the voltage-dependent inhibition of hK$_v$1.5 channels by AA, the current levels were measured at the end of depolarizing steps in the absence ($I_{control}$) and presence (I_{AA}) of AA, and the current ratio ($I_{AA}/I_{control}$, which represents the percentage of control) was plotted as a function of the test potentials (Figure 2D). The current reduction was steeply enhanced at potentials between −20 and +20 mV, which correspond to the voltage range of channel activation, as represented by the steep slope of the activation curve. As demonstrated in Figure 2E, the deactivating tail currents recorded at −40 mV before and after exposure to AA are reasonably well fitted with a single exponential function. AA significantly increased the deactivation time constants from 15.4 ± 2.3 ms to 40.1 ± 7.1 ms ($n = 10$; $P < 0.01$), showing that the deactivation of hK$_v$1.5 channel was delayed after exposure to AA. This phenomenon can be explained by the slow transition of the channel from an open to a closed state due to the slow dissociation of AA from the open state of hK$_v$1.5 channel during repolarization. AA also reduced the initial peak amplitudes of tail currents (Figure 2E). These two actions of AA produced a crossover of the tail current traces recorded in the absence and presence of AA, as has been reported for other blockers of hK$_v$1.5 channels (Snyders and Yeola, 1995; Valenzuela *et al.*, 1996; Yeola *et al.*, 1996; Perchenet and Clément-Chomienne, 2000; Decher *et al.*, 2006).

Effect of AA on the hK$_v$1.5 channel through extracellular sites independent of its metabolites and signalling pathways

Because AA can readily pass the cell membrane, we needed to determine whether the effect of AA on the hK$_v$1.5 channel is mediated through extracellular or intracellular sites. BSA itself cannot cross the membrane but has a potent capacity to bind free AA (Bojesen and Bojesen, 1994) and to thereby diminish the action of AA on ion channels (Liu *et al.*, 2001; Talavera *et al.*, 2004; Liu, 2007). BSA is therefore a useful tool for differentiating the site of AA action on

ion channels in various tissues, including the heart. As shown in Figure 3A, the external addition of BSA (0.1%) rapidly and almost totally reversed the AA (10 μM)-induced inhibition of $hK_v1.5$ current. This reversing effect of BSA (0.1%) was readily removed after the washout of BSA from the bath. In contrast, when BSA was added to the cell inside through a recording pipette, the external application of AA (10 μM) markedly reduced $hK_v1.5$ current (Figure 3B). Under this condition, the AA-induced current inhibition was almost totally reversed by further addition of BSA to the extracellular side. These observations are consistent with the view that AA affects $hK_v1.5$ channel through extracellular sites.

The metabolic products of AA produced by the action of COX, LOX and cytochrome P450 can modify the activity of some of ion channels (Meves, 2008). To address this question, the effects of potent inhibitors for three major metabolic cascades of AA were investigated. IDM (COX inhibitor, 10 μM), NDGA (LOX inhibitor, 50 μM) or ETYA (inhibitor of LOX, COX and cytochrome P450, 30 μM) was added to the inside of the cell through a recording pipette. Figure 3C shows that all three inhibitors failed to affect the AA-induced reduction of the $hK_v1.5$ current. Next, because AA affects some of the ion channels via PKC activation or through oxygen radical production (Linden and Routtenberg, 1989; Keyser and Alger, 1990), we examined the possible involvement of these signalling molecules in the AA-induced inhibition of $hK_v1.5$ current. As shown in Figure 3C, neither BIS-I (PKC inhibitor, 200 nM) nor SOD (oxygen radical scavenger, 100 $U \cdot mL^{-1}$) prevented the inhibitory action of AA on $hK_v1.5$ current, suggesting that neither PKC nor oxygen radicals are involved in the effect of AA on $hK_v1.5$ current.

Attenuation of AA-induced inhibition of $hK_v1.5$ channels with an alkaline external pH

Previous studies have shown that the $hK_v1.5$ channel is sensitive to changes in external pH (Trapani and Korn, 2003). Hence we examined the effect of external pH on the inhibitory action of AA. We first tested the effects of external pH (6.4, 7.7 and 8.0) on $hK_v1.5$ current in the experiments shown in Figure 4A and B. The amplitude of the $hK_v1.5$ current measured at +30 mV was decreased at pH 6.4 but increased at pH 8.0, whereas it was unaffected at pH 7.7. These responses of the $hK_v1.5$ current to external pH are qualitatively similar to the observations of a previous study (Trapani and Korn, 2003). Figure 4C shows superimposed current traces of the $hK_v1.5$ current recorded in the absence and presence of AA (10 μM) at an external pH 8.0. As summarized in Figure 4D, the inhibitory effect of AA on the $hK_v1.5$ current was significantly attenuated at external pH 8.0 compared with that at pH 7.4, but was not affected by external pH 6.4 and 7.7.

AA-induced inhibition of $hK_v1.5$ co-expressed with $K_v\beta1.3$

It has been reported that the $K_v\beta$ subunits $K_v\beta1.3$ and $K_v\beta2.1$ exhibit expression patterns that overlap with $hK_v1.5$ in human myocardium (Arias *et al.*, 2007; Ravens and Wettwer, 2011). In addition, heterologous expression experiments have shown that $K_v\beta1.3$ modifies the functional properties and pharmacological

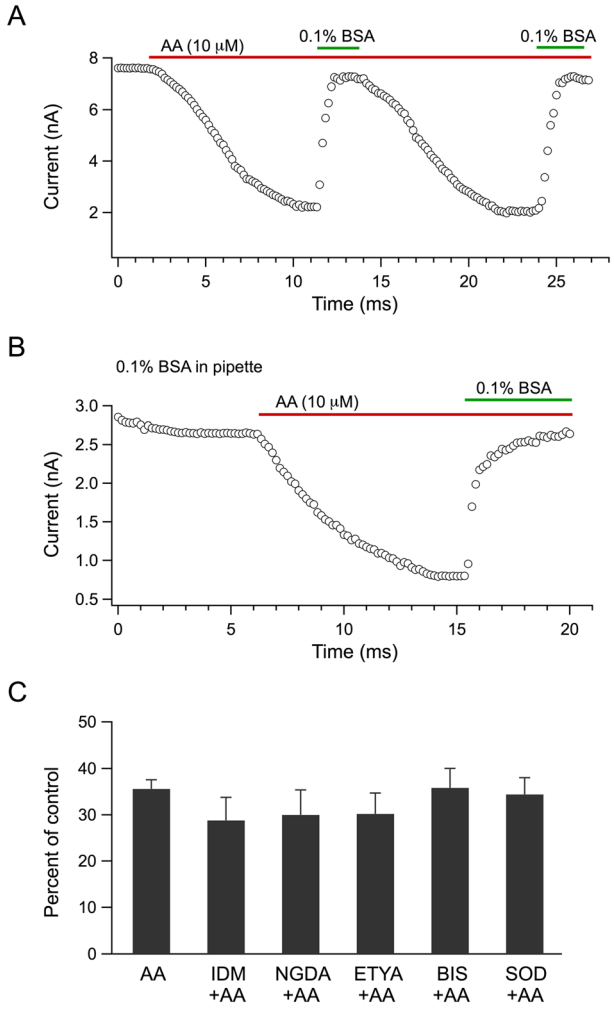

Figure 3

AA action on $hK_v1.5$ channel through extracellular sites independent of its metabolites and signalling pathways. (A) Time course of changes in the amplitude of $hK_v1.5$ current activated by depolarizing steps to +30 mV during the external application of AA (10 μM) and BSA (0.1%). AA and BSA were added at the time periods indicated by the horizontal bars. (B) Time course of changes in the amplitude of $hK_v1.5$ current in the presence of BSA (0.1%) in the pipette. AA (10 μM) and BSA (0.1%) were added extracellularly at the time periods indicated by the horizontal bars. (C) Effects of metabolic inhibitors of AA, a PKC inhibitor and oxygen radical scavenger on the AA-induced inhibition of $hK_v1.5$ channel. IDM (10 μM, $n = 5$), NDGA (50 μM, $n = 5$), ETYA (30 μM, $n = 4$) or SOD (100 $U \cdot mL^{-1}$, $n = 5$) was added to the cell inside through a recording pipette, whereas BIS-I (200 nM, $n = 5$) was applied to the bath solution.

sensitivity of $hK_v1.5$ (Uebele *et al.*, 1998; Gonzalez *et al.*, 2002; Arias *et al.*, 2007). We therefore examined the effects of co-expression of $K_v\beta1.3$ with $hK_v1.5$ on the inhibitory action of AA. As shown in Figure 5A, co-expression of $K_v\beta1.3$ with $hK_v1.5$ induced a fast current inactivation at +30 mV, as has previously been reported (Uebele *et al.*, 1998; Gonzalez *et al.*, 2002; Arias *et al.*, 2007). Subsequent addition of 10 μM AA also inhibited $hK_v1.5$ co-expressed with $K_v\beta1.3$. We measured the time course of current reduction during the application of 10 μM AA in $hK_v1.5$ alone and $hK_v1.5$ co-expressed with

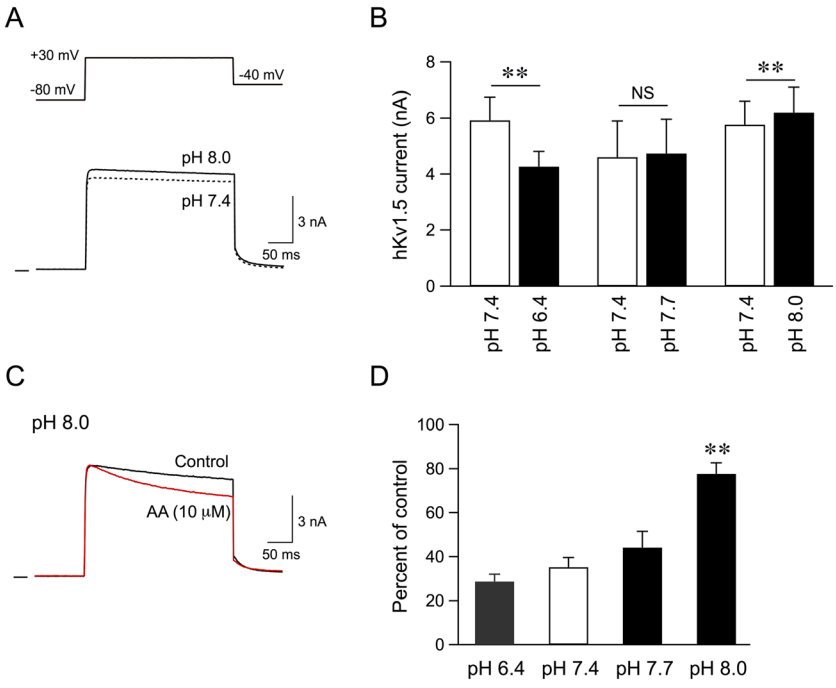

Figure 4

Effect of external pH on the AA-induced inhibition of hK$_v$1.5 channel. (A) Superimposed hK$_v$1.5 currents elicited by 300 ms depolarizing steps to +30 mV, during superfusion with bath solutions at pH 7.4 (dotted curve) and pH 8.0 (continuous curve). (B) Effect of external pH on the amplitude of hK$_v$1.5 current. The cells were initially superfused with a bath solution at pH 7.4 and then a bath solution at pH 6.4 ($n = 5$), pH 7.7 ($n = 5$) or pH 8.0 ($n = 8$). Note that the effect of only one test pH (6.4, 7.7 or 8.0) was examined in a given cell and that there were no significant differences in the amplitude of hK$_v$1.5 currents at pH 7.4 among three comparison groups for pH 6.4, pH 7.7 and pH 8.0. $^{**}P < 0.01$ compared with respective pH 7.4 group. (C) Superimposed current traces of hK$_v$1.5 activated by depolarizing voltage steps to +30 mV before and 8 min after exposure to 10 μM AA recorded at an external pH 8.0. (D) Inhibitory effect of 10 μM AA on hK$_v$1.5 channel at external pH 6.4, pH 7.4, pH 7.7 or pH 8.0. $^{**}P < 0.01$ compared with pH 7.4.

K$_v$β1.3. Whereas the degree of hK$_v$1.5 inhibition without or with K$_v$β1.3 co-expression was similar at 10 min after exposure to AA, the inhibitory effect of AA was enhanced by K$_v$β1.3 co-expression at 2 and 5 min after exposure to AA (Figure 5B). Thus, the co-assembly of K$_v$β1.3 with hK$_v$1.5 was found to appreciably affect the blocking action of AA on hK$_v$1.5 channels.

Effects of AA on mutant hK$_v$1.5 channels

Previous studies have shown that several amino acids located in the pore domain of hK$_v$1.5 channel form an important structural basis for drug binding (Yeola *et al.*, 1996; Decher *et al.*, 2004; Decher *et al.*, 2006; Eldstrom *et al.*, 2007; Wu *et al.*, 2009; Ravens and Wettwer, 2011). To investigate the possible binding sites for

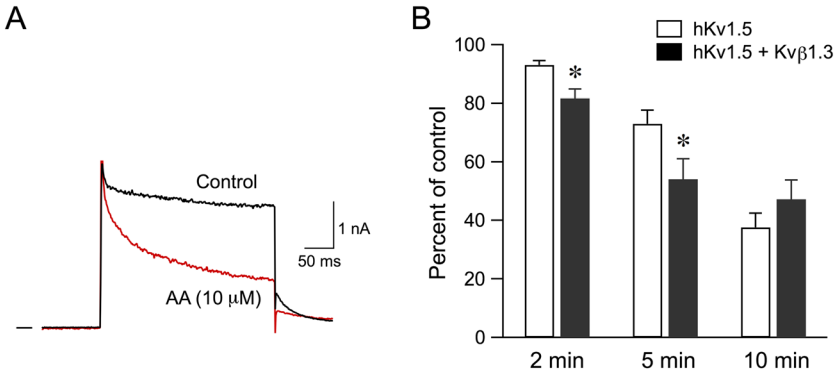

Figure 5

Inhibitory effect of AA on hK$_v$1.5 coexpressed with K$_v$β1.3. (A) Superimposed current traces of hK$_v$1.5 co-expressed with K$_v$β1.3, elicited by 300 ms depolarizing step to +30 mV before and 10 min after exposure to 10 μM AA. (B) AA-induced inhibition of hK$_v$1.5 without or with the co-expression of K$_v$β1.3, measured after 2, 5 and 10 min exposure to 10 μM AA respectively. $^{**}P < 0.01$ compared with hK$_v$1.5 at the same time point.

AA on $hK_v1.5$ channel, we introduced alanine (cysteine or valine) substitutions into 11 amino acids that reside within the pore domain. These amino acids are T462 and H463 (located at outer mouth of the pore helix), T479 and T480 (located at the base of selectivity filter), R487 (located at the external entryway of the pore), and A501, I502, I508, L510, V512 and V516 (located within S6 domain). All of these mutant channels (T462C, H463C, T479A, T480A, R487V, A501V, I502A, I508A, L510A, V512A and V516A) were functional and produce membrane currents in response to depolarizing steps, as previously demonstrated (Decher *et al.*, 2004; Decher *et al.*, 2006; Eldstrom *et al.*, 2007).

Figure 6A shows the effects of 10 μM AA on WT, T479A and T480A channels activated during depolarizing step to +30 mV. The degree of current inhibition by AA appeared to be rather constant in T480A during depolarizing steps, showing that the blocking action of AA on T480A does not exhibit typical properties of open-channel blockers. A similar observation has been described for the blocking action of S0100176 and vernakalant on the T480A mutant of $hK_v1.5$ channel (Decher *et al.*, 2004; Eldstrom *et al.*, 2007). As summarized in Figure 6B, the degree of inhibition by AA was significantly reduced in T480A but was significantly enhanced in T479A (the mutation at a neighbour residue of T480). We also determined the concentration–response relationships for the inhibitory effects of AA on T479A and T480A mutants as well as WT channels (Figure 6C); this yielded an IC_{50} of 2.5 ± 0.6 μM ($n = 6$) for T479A, 14.9 ± 1.0 μM ($n = 6$) for T480A and 6.1 ± 0.6 μM for WT ($n = 10$). This analysis again confirmed that T480A was less sensitive, while T479A was more sensitive to inhibition by AA, in comparison with the WT channel.

Figure 7A shows representative results of the inhibitory effects of 10 μM AA on T462C, H463C and V512A mutants of $hK_v1.5$ channel. Figure 7B summarizes the degree of current reduction by 10 μM AA in WT and the other nine mutant channels. The inhibitory effect of AA was significantly reduced in H463C, R487V, I502A, I508A, V512A and V516A mutants but not in T462C, A501V and L510A mutants, compared with WT channels. We further constructed the concentration–response relationships for the inhibitory effect of AA on H463C and V512A mutant channels (Figure 7C); this yielded an IC_{50} of 30.8 ± 1.6 μM ($n = 6$) for H463C, and 24.9 ± 1.9 μM ($n = 6$) for V512A. This finding again supports the view that the inhibitory effect of AA was significantly attenuated in H463C and V512A mutants, in comparison with the WT channel.

Docking simulation for AA binding to the $K_v1.5$ channel

We finally conducted a docking simulation study to investigate the putative binding site(s) of AA in an open-state model of the $K_v1.5$ channel. An energy-minimized docking procedure detects two stable docking conformations of AA in the channel (Figure 8). AA binds between the inter-subunits and extends to the external entryway of the pore, where H463 and R487 are predicted to interact with AA (Figure 8A). AA also binds to the inside of the pore region where T480, I508, V512 and V516 are predicted to interact with AA (Figure 8B). Thus, the present docking simulation is in reasonable agreement with the experimental results obtained using site-directed mutagenesis combined with patch-clamp experiments (Figures 6 and 7).

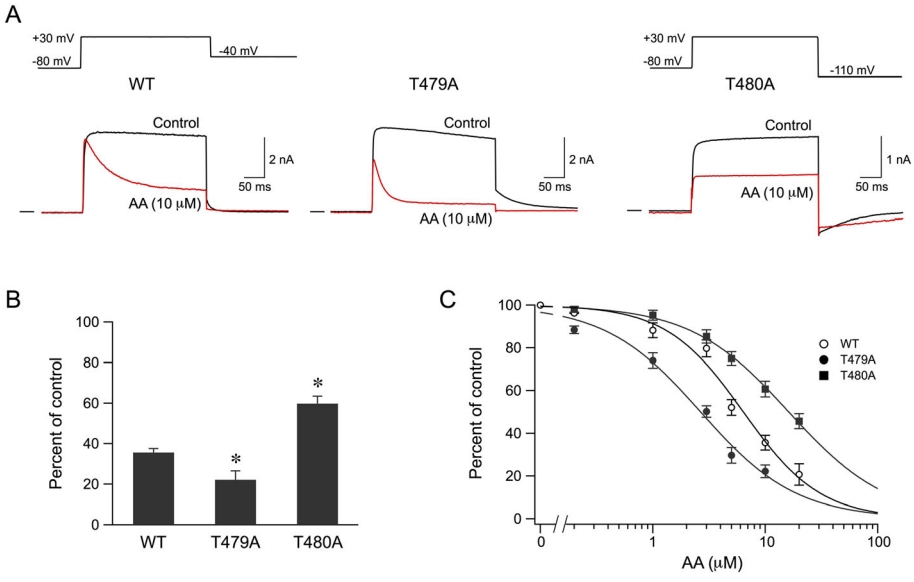

Figure 6

Effects of AA on $hK_v1.5$ channels mutated at the base of the selectivity filter. (A) Representative current traces recorded form WT and mutant channels (T479A and T480A) during 300 ms depolarizing steps to +30 mV, before and during exposure to 10 μM AA. (B) Inhibitory effect of 10 μM AA on WT, T479A and T480A mutant channels of $hK_v1.5$. *$P < 0.05$ compared with WT. (C) Concentration–response relationships for the inhibitory effect of AA on WT, T479A and T480A channels of $hK_v1.5$, measured at the end of a depolarizing step to +30 mV. Smooth curves through the data points represent a least-squares fit of Hill equation. Note that whereas the IC_{50} value for T480A (14.9 ± 1.0 μM, $n = 6$) is significantly larger than that for WT (6.1 ± 0.6 μM, $n = 10$), IC_{50} value for T479A (2.5 ± 0.6 μM, $n = 6$) is significantly smaller than that for WT.

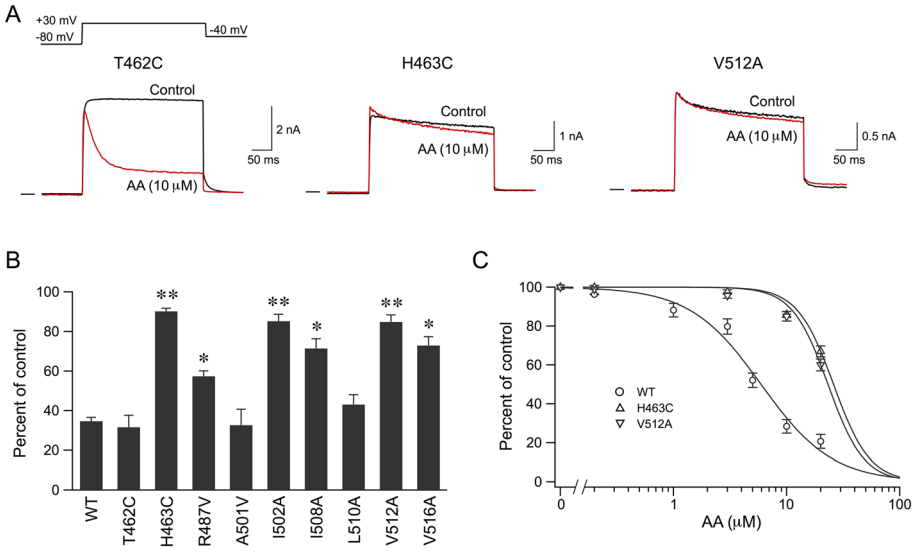

Figure 7

Effects of AA on hK$_v$1.5 channels mutated at the outer mouth of the pore helix, the external entryway of the pore and within S6. (A) Superimposed current traces recorded form T462C, H463C and V512A during 300 ms depolarizing step to +30 mV, before and during exposure to 10 μM AA. (B) Inhibitory effect of AA on WT and nine mutant channels. *$P < 0.05$ and **$P < 0.01$ compared with WT. (C) Concentration–response relationships for the inhibitory effect of AA on WT, H463C and V512A mutant channels of hK$_v$1.5, measured at the end of a depolarizing step to +30 mV. Note that IC$_{50}$ values for H463C (30.8 ± 1.6 μM, $n = 6$) and for V512A (24.9 ± 1.9 μM, $n = 6$) are significantly larger than IC$_{50}$ value for WT (6.1 ± 0.6 μM, $n = 10$).

Discussion

In the present study it was demonstrated that AA reversibly inhibits the hK$_v$1.5 current in a concentration-dependent manner with an average IC$_{50}$ of 6.1 μM (Figure 1B), which is smaller than that (21 μM) previously reported for the mK$_v$1.5 current (Honoré *et al.*, 1994). AA acts on hK$_v$1.5 channel as an open-channel blocker, which is supported by the following observations: (i) AA minimally affected the initial current levels at the onset of depolarization but progressively

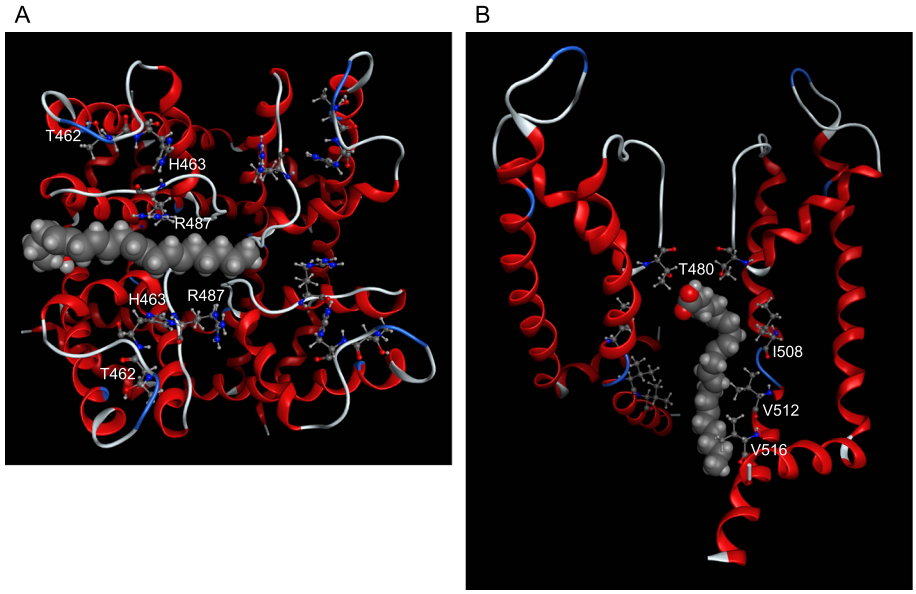

Figure 8

A docking simulation for AA binding to the K$_v$1.5 open-channel model. (A) A top view of the inter-subunit binding of AA with extension to the external entryway of the pore. (B) A side view of the pore region binding of AA. Two opposing pore domains are shown for clarity. AA is described as a space-fill model for panels A and B.

reduced the current during the depolarizing steps (Figures 1A and 2A); (ii) AA-induced inhibition of $hK_v1.5$ channel was evident at potentials positive to −20 mV, which corresponded to the voltage range of channel opening (Figure 2D); and (iii) AA significantly decelerated the current deactivation, leading to the crossover of tail currents (Figure 2E). These open-channel blocking properties are widely reported for anti-arrhythmic and pharmacological agents that act on $hK_v1.5$ channels, such as clofilium (Snyders and Yeola, 1995), quinidine (Yeola *et al.*, 1996), zatebradine (Valenzuela *et al.*, 1996), papaverine (Choe *et al.*, 2003), S0100176 (Decher *et al.*, 2004), AVE0118 (Decher *et al.*, 2006) and LY294002 (Wu *et al.*, 2009).

It has been reported that the electrophysiological effects of AA on the human ether *á go-go* K^+ channel, $K_{ir}2.3$ channel and L-type Ca^{2+} channel are mainly caused by an effect on an extracellular site of the cell membrane (Liu *et al.*, 2001; Gavrilova-Ruch *et al.*, 2007; Liu, 2007). In the present investigation, the experimental findings also indicate that AA itself acts on $hK_v1.5$ channel at the extracellular site (Figure 3). It should be noted that the onset and washout for the action of AA on $hK_v1.5$ channel developed rather slowly (Figure 1C) despite it acting on an extracellular site. Although the precise mechanism remains unknown, the inhibitory action of AA and its derivatives on ion channels has been demonstrated to have a similarly slow time course (Talavera *et al.*, 2004; Barana *et al.*, 2010).

Although AA itself has been demonstrated to affect various ion channels, the molecular determinants mediating the action of AA have yet to be fully elucidated. However, a previous study clearly demonstrated that phosphorylation of serine-4 in the NH_2 terminus plays a key role in mediating the inhibitory effects of AA on the ROMK ($K_{ir}1.1$) channel (Macica *et al.*, 1998). It was also found that a charged region (KKTKEE) near the proximal COOH terminus is structurally important for determining the AA sensitivity of the TREK-2 ($K_{2P}10.1$) channel (Kim *et al.*, 2001). Moreover, a site-directed mutagenesis study revealed that the pore-lining amino acids T250 (just prior to the K^+ selectivity filter GYG) and V275 (within S6 domain) in the human intermediate conductance, Ca^{2+}-activated K^+ channel (hKCa4) confers inhibition of the channel by AA (Hamilton *et al.*, 2003). In the present study it was found that several amino acids such as H463 (located at outer mouth of the pore helix), T480 (located at the base of selectivity filter), R487 (located at the external entryway of the pore), and I502, I508, V512 and V516 (located within S6 domain) are crucial for mediating the AA-induced inhibition of the $hK_v1.5$ channel (Figures 6 and 7). Because T480 in the $hK_v1.5$ channel is equivalent to T250 in the hKCa4 channel, threonine located at the base of the selectivity filter is important in conferring AA sensitivity to both the $hK_v1.5$ and hKCa4 channels.

The present study also found that while T480A decreases the sensitivity to AA inhibition, mutation of its neighbour amino acid T479 enhances AA inhibition (Figure 6). Although the precise mechanism remains to be fully understood, there might be some positive steric effects of T479A mutation on the neighbouring T480 or on other potent AA binding sites. Interestingly, a similar enhancement of $hK_v1.5$ blockade by vernakalant and flecainide has been noted in T479A mutant channel (Eldstrom *et al.*, 2007).

Previous studies have shown that I502, I508, V512 and V516 are important for mediating the blocking action of various drugs on $hK_v1.5$ channel, such as S0100176 and AVE0118 (Decher *et al.*, 2004; Decher *et al.*, 2006). Similarly, R487 and H463 are also important for the blocking actions of protons (Kehl *et al.*, 2002), drugs (Rezazadeh *et al.*, 2006; Gong *et al.*, 2008) and AA derivative *N*-arachidonoylethanolamine (Barana *et al.*, 2010). Based on the crystal structure of $K_v1.2$, T480, I508, V512 and V516 are predicted to face toward the inner cavity of the channel, whereas I502 is positioned away from the central cavity of the pore and forms a hydrophobic interface with the adjacent S5 domain (Decher *et al.*, 2006; Eldstrom *et al.*, 2007; Tikhonov and Zhorov, 2014). The present docking simulation study predicted that H463, T480, R487, I508, V512 and V516, but not I502, interact with AA (Figure 8). However, the mutation of I502 was found to substantially reduce the degree of $hK_v1.5$ channel block by AA (Figure 7) and other drugs (Decher *et al.*, 2004; Decher *et al.*, 2006; Eldstrom *et al.*, 2007; Wu *et al.*, 2009). Several mechanisms may be postulated to explain the functional role of I502 in the blocking action of AA: (i) the mutation of I502 affects the blocking actions of compounds through conformational changes of the pore (Eldstrom *et al.*, 2007) and (ii) hydrophobic moieties of the compound protrude into hydrophobic subunit interfaces and thereby approach the I502 residue (Tikhonov and Zhorov, 2014).

It has been proposed that while the lipophilic hydrocarbon chain in AA interacts with hydrophobic transmembrane domains of the channel proteins, the negative charge of the carboxyl group in AA interacts ionically with the positively charged amino acid residues of channel protein (Kang and Leaf, 1996). In the present study, we demonstrated that an alkaline external pH significantly reduced the sensitivity of $hK_v1.5$ channel to inhibiton by AA (Figure 4D). It is generally accepted that the environmental pH affects the degree of hydrophobicity in AA. In addition, the activation of $hK_v1.5$ channels is sensitive to changes in external pH (Trapani and Korn, 2003). These pH-dependent changes in the properties of both AA and $hK_v1.5$ channel might underlie the attenuation of the inhibition of $hK_v1.5$ channel by AA in an alkaline pH of 8.0.

In a previous clinical trial it was reported that the incidence of AF following coronary artery bypass graft surgery is less in patients with higher levels of AA in plasma phospholipids, suggesting that AA may play an important role in preventing the development of AF (Skuladottir *et al.*, 2011). It is probable that AA-induced inhibition of $hK_v1.5$ channels could prolong the APD and ERP in human atrium and thereby mediate the anti-arrhythmic effect of AA. However, APD critically depends on a delicate balance between several inward and outward currents, and AA has various effects on other ionic currents that regulate APD in the heart, such as the voltage-gated Na^+ channel, Ca^{2+} channel and HERG K^+ channels (Ding *et al.*, 2000; Guizy *et al.*, 2005; Liu, 2007). AA therefore could produce complicated effects on overall atrial excitability. It is, however, expected that a simultaneous inhibitory effect of AA on $hK_v1.5$ channels counteracts the APD-shortening effect mediated through inhibition of voltage-gated Na^+ and Ca^{2+} channels by AA. Future studies are required to elucidate the electrophysiological basis for the possible anti-arrhythmic action of AA in human atrium.

In conclusion, the present study provides experimental evidence showing that several amino acids in the pore domain (H463, T480, R487, I502, I508, V512 and V516) confer the sensitivity of the $hK_v1.5$ channel to AA. This information may help investigate the molecular determinants for the action of other polyunsaturated fatty acids on $hK_v1.5$ channels and provide new directions for future development of selective blockers of the $hK_v1.5$ channel.

Acknowledgement

This study was supported by a Grant-in-Aid for Scientific Research (C) (no. 25460287 to H. M.) from The Japan Society for the Promotion of Science (Tokyo, Japan).

Author contributions

W. -G. D. and H. M. designed the experiments. J. -Y. B., W. -G. D., A. K. and T. S. conducted the experiments. J. -Y. B., W. -G. D., A. K., T. S. and H. M. participated in the data interpretation. J.-Y. B., W. -G. D., A. K., T. S. and H. M. wrote the manuscript. J. -Y. B., W. -G. D., A. K., T. S. and H. M. approved the final manuscript.

Conflict of interest

The authors declare no conflicts of interest in association with the present study.

References

Alexander SPH, Benson HE, Faccenda E, Pawson AJ, Sharman JL, Catterall WA *et al.* (2013a). The concise guide to PHARMACOLOGY 2013/14: ion channels. Br J Pharmacol 170: 1607–1651.

Alexander SPH, Benson HE, Faccenda E, Pawson AJ, Sharman JL, Spedding M *et al.* (2013b). The concise guide to PHARMACOLOGY 2013/14: enzymes. Br J Pharmacol 170: 1797–1867.

Arias C, Guizy M, David M, Marzian S, Gonzalez T, Decher N *et al.* (2007). Kvβ1.3 reduces the degree of stereoselective bupivacaine block of Kv1.5 channels. Anesthesiology 107: 641–651.

Barana A, Amorós I, Caballero R, Gómez R, Osuna L, Lillo MP *et al.* (2010). Endocannabinoids and cannabinoid analogues block cardiac hKv1.5 channels in a cannabinoid receptor-independent manner. Cardiovasc Res 85: 56–67.

Bojesen IN, Bojesen E (1994). Binding of arachidonate and oleate to bovine serum albumin. J Lipid Res 35: 770–778.

Brash AR (2001). Arachidonic acid as a bioactive molecule. J Clin Invest 107: 1339–1345.

Chien KR, Han A, Sen A, Buja LM, Willerson JT (1984). Accumulation of unesterified arachidonic acid in ischemic canine myocardium. Relationship to a phosphatidylcholine deacylation-reacylation cycle and the depletion of membrane phospholipids. Circ Res 54: 313–322.

Choe H, Lee YK, Lee YT, Ko SH, Joo CU, Kim MH *et al.* (2003). Papaverine blocks hKv1.5 channel current and human atrial ultrarapid delayed rectifier K^+ currents. J Pharmacol Exp Ther 304: 706–712.

Decher N, Kumar P, Gonzalez T, Pirard B, Sanguinetti MC (2006). Binding site of a novel Kv1.5 blocker: a "foot in the door" against atrial fibrillation. Mol Pharmacol 70: 1204–1211.

Decher N, Pirard B, Bundis F, Peukert S, Baringhaus KH, Busch AE *et al.* (2004). Molecular basis for Kv1.5 channel block: conservation of drug binding sites among voltage-gated K^+ channels. J Biol Chem 279: 394–400.

Ding GL, Hu D, Liu X, Li J, Zhang H, Li C (2000). Suppression of sodium current by arachidonic acid in atrial myocytes from patients with coronary heart disease. Pacing Clin Electrophysiol 23: 1820–1822.

Eldstrom J, Wang Z, Xu H, Pourrier M, Ezrin A, Gibson K *et al.* (2007). The molecular basis of high-affinity binding of the antiarrhythmic compound vernakalant (RSD1235) to Kv1.5 channels. Mol Pharmacol 72: 1522–1534.

Fedida D, Wible B, Wang Z, Fermini B, Faust F, Nattel S *et al.* (1993). Identity of a novel delayed rectifier current from human heart with a cloned K^+ channel current. Circ Res 73: 210–216.

Feng J, Wible B, Li G-R, Wang Z, Nattel S (1997). Antisense oligodeoxynucleotides directed against Kv1.5 mRNA specifically inhibit ultrarapid delayed rectifier K^+ current in cultured adult human atrial myocytes. Circ Res 80: 572–579.

Gavrilova-Ruch O, Schonherr R, Heinemann SH (2007). Activation of hEAG1 potassium channels by arachidonic acid. Pflügers Arch 453: 891–903.

Gong YZ, Ding WG, Wu J, Tsuji K, Horie M, Matsuura H (2008). Cinnamyl-3,4-dihydroxy-alpha-cyanocinnamate and nordihydroguaiaretic acid inhibit human Kv1.5 currents independently of lipoxygenase. Eur J Pharmacol 600: 18–25.

Gonzalez T, Navarro-Polanco R, Arias C, Caballero R, Moreno I, Delpon E *et al.* (2002). Assembly with the Kvβ1.3 subunit modulates drug block of hKv1.5 channels. Mol Pharmacol 62: 1456–1463.

Goto J, Kataoka R, Muta H, Hirayama N (2008). ASEDock-docking based on alpha spheres and excluded volumes. J Chem Inf Model 48: 583–590.

Guizy M, Arias C, David M, Gonzalez T, Valenzuela C (2005). ω-3 and ω-6 polyunsaturated fatty acids block *HERG* channels. Am J Physiol 289: C1251–C1260.

Halgren T (1996). Merck molecular force field. I. Basis, form, scope, parameterization, and performance of MMFF94. J Comput Chem 17: 490–519.

Halgren T (1999). MMFF VI. MMFF94s option for energy minimization studies. J Comput Chem 20: 720–729.

Hamilton KL, Syme CA, Devor DC (2003). Molecular localization of the inhibitory arachidonic acid binding site to the pore of hIK1. J Biol Chem 278: 16690–16697.

Honoré E, Barhanin J, Attali B, Lesage F, Lazdunski M (1994). External blockade of the major cardiac delayed-rectifier K^+ channel (Kv1.5) by polyunsaturated fatty acids. Proc Natl Acad Sci U S A 91: 1937–1941.

Kang JX, Leaf A (1996). Evidence that free polyunsaturated fatty acids modify Na^+ channels by directly binding to the channel proteins. Proc Natl Acad Sci U S A 93: 3542–3546.

Kehl SJ, Eduljee C, Kwan DC, Zhang S, Fedida D (2002). Molecular determinants of the inhibition of human Kv1.5 potassium currents by external protons and Zn^{2+}. J Physiol 541: 9–24.

Keyser DO, Alger BE (1990). Arachidonic acid modulates hippocampal calcium current via protein kinase C and oxygen radicals. Neuron 5: 545–553.

Kim D, Pleumsamran A (2000). Cytoplasmic unsaturated free fatty acids inhibit ATP-dependent gating of the G protein-gated K^+ channel. J Gen Physiol 115: 287–304.

Kim Y, Gnatenco C, Bang H, Kim D (2001). Localization of TREK-2 K^+ channel domains that regulate channel kinetics and sensitivity to pressure, fatty acids and pH_i. Pflügers Arch 442: 952–960.

Linden DJ, Routtenberg A (1989). cis-Fatty acids, which activate protein kinase C, attenuate Na^+ and Ca^{2+} currents in mouse neuroblastoma cells. J Physiol 419: 95–119.

Liu SJ (2007). Inhibition of L-type Ca^{2+} channel current and negative inotropy induced by arachidonic acid in adult rat ventricular myocytes. Am J Physiol 293: C1594–C1604.

Liu SJ, McHowat J (1998). Stimulation of different phospholipase A_2 isoforms by TNF-α and IL-1β in adult rat ventricular myocytes. Am J Physiol 275: H1462–H1472.

Liu Y, Liu D, Heath L, Meyers DM, Krafte DS, Wagoner PK *et al.* (2001). Direct activation of an inwardly rectifying potassium channel by arachidonic acid. Mol Pharmacol 59: 1061–1068.

Long SB, Cambell EB, Mackinnon R (2005). Crystal structure of a mammalian voltage-dependent *Shaker* family K^+ channel. Science 309: 897–903.

Lu T, Ye D, Wang X, Seubert JM, Graves JP, Bradbury JA *et al.* (2006). Cardiac and vascular K_{ATP} channels in rats are activated by endogenous epoxyeicosatrienoic acids through different mechanisms. J Physiol 575: 627–644.

Macica CM, Yang Y, Lerea K, Hebert SC, Wang W (1998). Role of the NH_2 terminus of the cloned renal K^+ channel, ROMK1, in arachidonic acid-mediated inhibition. Am J Physiol 274: F175–F181.

Mays DJ, Foose JM, Philipson LH, Tamkun MM (1995). Localization of the Kv1.5 K^+ channel protein in explanted cardiac tissue. J Clin Invest 96: 282–292.

McHowat J, Liu S, Creer MH (1998). Selective hydrolysis of plasmalogen phospholipids by Ca^{2+}-independent PLA_2 in hypoxic ventricular myocytes. Am J Physiol 274: C1727–C1737.

Meves H (2008). Arachidonic acid and ion channels: an update. Br J Pharmacol 155: 4–16.

Pawson AJ, Sharman JL, Benson HE, Faccenda E, Alexander SP, Buneman OP *et al.* (2014). The IUPHAR/BPS Guide to PHARMACOLOGY: an expert-driven knowledgebase of drug targets and their ligands. Nucleic Acids Research 42 (Database Issue): D1098–D1106.

Perchenet L, Clément-Chomienne O (2000). Characterization of mibefradil block of the human heart delayed rectifier hKv1.5. J Pharmacol Exp Ther 295: 771–778.

Petit-Jacques J, Hartzell HC (1996). Effect of arachidonic acid on the L-type calcium current in frog cardiac myocytes. J Physiol 493: 67–81.

Ravens U, Cerbai E (2008). Role of potassium currents in cardiac arrhythmias. Europace 10: 1133–1137.

Ravens U, Wettwer E (2011). Ultra-rapid delayed rectifier channels: molecular basis and therapeutic implications. Cardiovasc Res 89: 776–785.

Rezazadeh S, Claydon TW, Fedida D (2006). KN-93 (2-[N-(2-hydroxyethyl)]-N-(4-methoxybenzenesulfonyl)]amino-N-(4-chlorocinnamyl)-N -methylbenzylamine), a calcium/calmodulin-dependent protein kinase II inhibitor, is a direct extracellular blocker of voltage-gated potassium channels. J Pharmacol Exp Ther 317: 292–299.

Skuladottir GV, Heidarsdottir R, Arnar DO, Torfason B, Edvardsson V, Gottskalksson G *et al.* (2011). Plasma n-3 and n-6 fatty acids and the incidence of atrial fibrillation following coronary artery bypass graft surgery. Eur J Clin Invest 41: 995–1003.

Snyders DJ, Yeola SW (1995). Determinants of antiarrhythmic drug action. Electrostatic and hydrophobic components of block of the human cardiac hKv1.5 channel. Circ Res 77: 575–583.

Talavera K, Staes M, Janssens A, Droogmans G, Nilius B (2004). Mechanism of arachidonic acid modulation of the T-type Ca^{2+} channel α_{1G}. J Gen Physiol 124: 225–238.

Tikhonov DB, Zhorov BS (2014). Homology modeling of Kv1.5 channel block by cationic and electroneutral ligands. Biochim Biophys Acta 1838: 978–987.

Trapani JG, Korn SJ (2003). Effect of external pH on activation of the Kv1.5 potassium channel. Biophys J 84: 195–204.

Uebele VN, England SK, Gallagher DJ, Snyders DJ, Bennett PB, Tamkun MM (1998). Distinct domains of the voltage-gated K^+ channel Kvβ1.3 β-subunit affect voltage-dependent gating. Am J Physiol 274: C1485–C1495.

Valenzuela C, Delpon E, Franqueza L, Gay P, Perez O, Tamargo J *et al.* (1996). Class III antiarrhythmic effects of zatebradine. Time-, state-, use-, and voltage-dependent block of hKv1.5 channels. Circulation 94: 562–570.

Wang Z, Fermini B, Nattel S (1993). Delayed rectifier outward current and repolarization in human atrial myocytes. Circ Res 73: 276–285.

Wettwer E, Hala O, Christ T, Heubach JF, Dobrev D, Knaut M *et al.* (2004). Role of I_{Kur} in controlling action potential shape and contractility in the human atrium: influence of chronic atrial fibrillation. Circulation 110: 2299–2306.

Wu J, Ding WG, Matsuura H, Tsuji K, Zang WJ, Horie M (2009). Inhibitory actions of the phosphatidylinositol 3-kinase inhibitor LY294002 on the human Kv1.5 channel. Br J Pharmacol 156: 377–387.

Yedgar S, Cohen Y, Shoseyov D (2006). Control of phospholipase A2 activities for the treatment of inflammatory conditions. Biochim Biophys Acta 1761: 1373–1382.

Yeola SW, Rich TC, Uebele VN, Tamkun MM, Snyders DJ (1996). Molecular analysis of a binding site for quinidine in a human cardiac delayed rectifier K^+ channel. Role of S6 in antiarrhythmic drug binding. Circ Res 78: 1105–1114.